Journal of Coastal Research	29	6	1257–1272	Coconut Creek, Florida	November 2013

On the Accuracy of SeaWiFS Ocean Color Data Products on the West Florida Shelf

Jennifer P. Cannizzaro[†], Chuanmin Hu[†], Kendall L. Carder[‡], Christopher R. Kelble[§], Nelson Melo[§,††], Elizabeth M. Johns[§], Gabriel A. Vargo[†], and Cynthia A. Heil[‡‡]

[†]College of Marine Science
University of South Florida
140 7th Avenue South
St. Petersburg, FL 33701, U.S.A.
jpatch@mail.usf.edu

[‡]SRI International
450 8th Avenue South
St. Petersburg, FL 33701, U.S.A.

[§]U.S. NOAA Atlantic Oceanographic & Meteorological Laboratory
4301 Rickenbacker Causeway
Miami, FL 33149, U.S.A.

[††]Cooperative Institute for Marine and Atmospheric Studies (CIMAS)
University of Miami
4600 Rickenbacker Causeway
Miami, FL 33149, U.S.A.

[‡‡]Bigelow Laboratory for Ocean Sciences
180 McKown Point Road
West Boothbay Harbor, ME 04575, U.S.A.

www.cerf-jcr.org

www.JCRonline.org

ABSTRACT

Cannizzaro, J.P.; Hu, C.; Carder, K.L.; Kelble, C.R.; Melo, N.; Johns, E.M.; Vargo, G.A., and Heil, C.A., 2013. On the accuracy of SeaWiFS ocean color data products on the West Florida Shelf. *Journal of Coastal Research,* 29(6), 1257–1272. Coconut Creek (Florida), ISSN 0749-0208.

Despite the importance of the West Florida Shelf (WFS) on regional ecology and local economy, systematic shelf-wide assessment of the ocean biology has not been conducted, primarily because of budgetary limitations for routine field campaigns and unknown accuracy of satellite-based data products. Here, using shipboard spectral normalized water-leaving radiance ($nL_w[\lambda]$) data and chlorophyll-a concentrations (Chl-a) collected regularly during two multiyear field programs spanning >10 years, the accuracies of Sea-viewing Wide Field-of-view Sensor (SeaWiFS) standard data products were evaluated. The *in situ* data covered a wide dynamic range, with about one order of magnitude in $nL_w(490)$ (0.47 to 4.01 mW cm^{-2} μm^{-1} sr^{-1}) and two orders of magnitude in Chl-a (0.07 to 10.6 mg m^{-3}). Near-concurrent *in situ* and satellite $nL_w(\lambda)$ data showed absolute percent differences (APD) increasing from 7–9% to 10–14% when data with elevated aerosol optical thicknesses at 865 nm (τ_a865) were included. Most of this uncertainty, however, canceled in the maximal blue-to-green reflectance band ratios traditionally used for estimating Chl-a. SeaWiFS OC4 Chl-a showed a root mean square (RMS) uncertainty of 0.106 for log-transformed data in waters offshore of the 20-m isobath that increased to 0.255 when all data were considered. The increased likelihood for nearshore SeaWiFS Chl-a greater than ~0.5 mg m^{-3} to be overestimated was shown to be caused by a variety of factors (colored dissolved organic matter [CDOM], suspended sediments, and bottom reflectance) that varied in both time and space. In the future, more sophisticated algorithms capable of taking these factors into consideration are required to improve remote determinations of Chl-a in nearshore waters of the WFS.

ADDITIONAL INDEX WORDS: *SeaWiFS, chlorophyll a, algorithm, atmospheric correction, suspended sediments, bottom reflectance, harmful algal blooms, colored dissolved organic matter, Gulf of Mexico.*

INTRODUCTION

Located in the eastern Gulf of Mexico, the West Florida Shelf (WFS) is home to rich and productive ecosystems supporting diverse populations of neritic and benthic organisms. Economically and ecologically, this region is highly important given the numerous commercial and recreational fisheries as well as tourism, shipping, and mining/petroleum industries located here. Understanding the ecological state of the WFS as well as its response to climate variability and anthropogenic influence requires sustained, routine measurements of a suite of physical, optical, and biogeochemical variables. Of particular importance is the chlorophyll-a concentration (Chl-a in mg m^{-3}) in the water column, as it is an indicator of phytoplankton biomass that can be used for determining the trophic state. Despite enormous past effort in measuring this fundamental biological variable using a variety of means including field (*e.g.* discrete water sample analysis and three-dimensional surveys using gliders) and satellite measurements, the spatial and temporal distribution patterns of Chl-a are still yet to be quantified in this region. This is primarily because the field measurements typically lack sufficient measurement frequency and coverage to yield statistically meaningful results, and more frequent and synoptic satellite measurements may contain substantial errors on the WFS attributable to its optical complexity.

DOI: 10.2112/JCOASTRES-D-12-00223.1 received 2 November 2012; accepted in revision 21 December 2012; corrected proofs received 12 February 2013.
Published Pre-print online 28 March 2013.

Over the past several decades, satellite ocean color radiometry has proven to be highly useful for examining spatial and temporal variability of near-surface phytoplankton biomass, as determined by Chl-a, on both global and regional scales (*e.g.* Gregg and Conkright, 2002; Morey, Dukhovskoy, and Bourassa, 2009; Yoder and Kennelly, 2003). The synoptic nature of such data as provided by sensors, including the U.S. National Aeronautics and Space Administration (NASA) Sea-viewing Wide Field-of-view Sensor (SeaWiFS; 1997–2011), Moderate Resolution Imaging Spectroradiometer (MODIS; 2000–present), and Visible Infrared Imager Radiometer Suite (VIIRS; 2011–present) and the European Space Agency (ESA) Medium Resolution Imaging Spectrometer (MERIS; 2002–12), has made this possible. Such sensors are capable of collecting high resolution (0.25–1 km) data across wide swaths (>1000 km) of land and ocean on a near-daily basis.

While Chl-a retrievals from satellite ocean color radiometry are generally successful in open ocean waters where optical properties are dominated by phytoplankton and their direct degradation products (McClain, Feldman, and Hooker, 2004), retrievals in more optically complex coastal waters may contain substantial uncertainty. Accurate Chl-a retrievals depend on both atmospheric correction algorithms (to convert satellite at-sensor radiance to normalized water-leaving radiance, $nL_w[\lambda]$, which is equivalent to remote sensing reflectance, $R_{rs}[\lambda]$) and bio-optical algorithms (to convert $R_{rs}[\lambda]$ to Chl-a). While atmospheric correction procedures have improved greatly in recent years with the addition of more sophisticated algorithms for dealing with high turbidity and aerosol changes (Ahmad *et al.*, 2010; Hu, Carder, and Müller-Karger, 2000; Ruddick, Ovidio, and Rijkeboer, 2000; Siegel *et al.*, 2000; Stumpf *et al.*, 2003a; Wang and Shi, 2007), retrieval accuracies for $nL_w(\lambda)$ remain poor in coastal environments, with errors typically increasing with increased proximity to shore (Antoine *et al.*, 2008; Darecki and Stramski, 2004).

The default SeaWiFS Chl-a algorithm (OC4) in NASA's data processing software SeaDAS is empirical in nature, developed from best-fit relationships between *in situ* measurements of Chl-a and maximal blue-to-green $R_{rs}(\lambda)$ ratios (O'Reilly *et al.*, 2000). The underlying rationale is that $R_{rs}(\lambda)$ is approximately proportional to light backscattering divided by light absorption within the first optical depth (Gordon, Brown, and Jacobs, 1975; Morel and Prieur, 1977). While backscattering is largely spectrally independent, phytoplankton pigments dominated by Chl-a absorb blue light strongly and green light weakly, thus causing blue-to-green reflectance ratios to decrease when pigment concentrations increase.

The OC4 empirical algorithm was designed to derive Chl-a for phytoplankton-dominated waters, as it does not distinguish between all the various optically significant constituents (OSCs) in the water column that influence $R_{rs}(\lambda)$. Specifically, the algorithm has been shown to fail when colored dissolved organic matter (CDOM) from terrestrial outflow or scattering-rich sediments from wind-driven resuspension events do not co-vary with Chl-a (Carder *et al.*, 1991; Wozniak and Stramski, 2004). The algorithm can also fail in clear, shallow waters when light reflected from the bottom influences $R_{rs}(\lambda)$ (Cannizzaro and Carder, 2006; Dekker *et al.*, 2011).

While alternative semianalytical approaches for estimating Chl-a have been developed that can distinguish between major OSCs (*e.g.* phytoplankton pigments, CDOM, and suspended sediments) (Carder *et al.*, 1999; Garver and Siegel, 1997; Lyon *et al.*, 2004; Maritorena, Siegel, and Peterson, 2002), the algorithm parameterization oftentimes requires regional tuning in coastal waters (Garcia *et al.*, 2006). Furthermore, semianalytical algorithms are highly sensitive to atmospheric correction errors given their need for accurate $R_{rs}(\lambda)$ at shorter wavebands than those utilized by standard empirical approaches.

In summary, the ecological and economic importance of the WFS calls for a long-term Chl-a data record in order to determine coastal water quality, to assess fisheries, and to monitor harmful algal blooms (HABs). Increased demands placed on coastal resource and public health managers responsible for making best management decisions for protecting the environment and human health also necessitate the availability of timely and accurate Chl-a estimates, which may be achieved through integration of *in situ* and remote sensing efforts (Udy *et al.*, 2005). The accuracy of satellite-based Chl-a on the WFS, however, is largely unknown. For example, where, when, and how much shall we trust satellite-derived values? Thus, motivated by the high demand in long-term data and lack of sufficient information on data quality, we conducted this research with the following objectives:

(1) to assess the accuracies of SeaWiFS $nL_w(\lambda)$ and Chl-a estimated using the default OC4 algorithm on the WFS, and
(2) to better understand where, when, and why the default OC4 Chl-a algorithm performed well or poorly in these coastal waters.

DATA AND METHODS

In Situ Data

Shipboard data were obtained during two multiyear programs with intense field sampling campaigns on the central and southern portions of the WFS together spanning more than a decade (1998–2009) and nearly the entire lifetime of the SeaWiFS mission (Figures 1 and 2). Data were collected monthly as part of the Ecology and Oceanography of Harmful Algal Blooms (ECOHAB) program (June 1998–December 2001) on the central portion of the WFS between Tampa Bay (~27.6° N) and Charlotte Harbor (~26.7° N) and from the 10-m isobath offshore to the shelf break (~200-m isobath). Data were collected bimonthly as part of the U.S. NOAA Atlantic Oceanographic & Meteorological Laboratory's (AOML) South Florida Program (SFP) (February 2002–January 2009) during regional field surveys on the southern portion of the WFS between Charlotte Harbor and the Florida Keys (~24.6° N) and shoreward of the 40-m isobath.

During each field survey, water samples were collected at predetermined station locations and depths using Niskin bottles mounted on rosette samplers. Duplicate samples were filtered immediately through Whatman GF/F filters for fluorometric determinations of Chl-a (Holm-Hansen *et al.*,

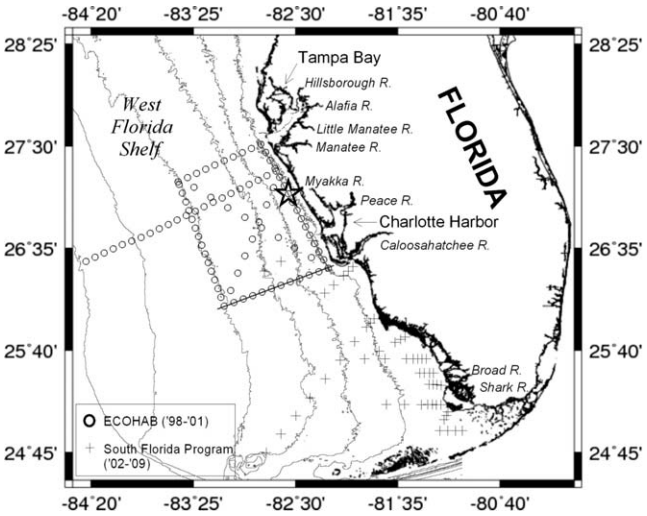

Figure 1. Map of station locations on the West Florida Shelf for the ECOHAB monthly cruises (1998–2001) (○) and South Florida Program bimonthly cruises (2002–2009) (+). Bathymetric lines representing the 10-, 20-, 30-, 50-, 100-, and 200-m isobaths are overlaid on the map. The star identifies the location of ECOHAB station 78 (27.089° N, 82.546° W). Locations of the alongshore and across-shore transects from which satellite data were extracted are also shown (solid lines).

1965). For the ECOHAB cruises, the filters were extracted immediately in 100% methanol at –20°C for 2–5 days until chlorophyll concentrations were measured using a Turner Designs 10-AU field fluorometer. During SFP cruises, filters were stored in liquid nitrogen and then transferred to a –80°C ultrafreezer upon return to the laboratory. Within 1 month of collection, these filters were extracted in a 60 : 40 90% acetone to dimethyl sulfoxide mixture (Shoaf and Lium, 1976) for 16 hours at 5°C. Chlorophyll concentrations were then measured using a Turner Designs TD-700 fluorometer.

Because the satellite-detected ocean light is a weighted integration of the upper water column, *in situ* chlorophyll concentrations were optically weighted to the penetration depth (z_{90}) (Gordon, 1992) as follows:

$$\text{Chl–a}_{\text{weighted}} = \frac{\int_0^{z_{90}} g(z)\text{Chl–a}(z)dz}{\int_0^{z_{90}} g(z)dz}, \quad (1)$$

where Chl-a$_{\text{weighted}}$ is the weighted Chl-a value, Chl-a(z) is the chlorophyll concentration at depth z, and the weighting factor $g(z)$ is given by

$$g(z) = \exp\left[-2\int_0^z K_d(z')dz'\right], \quad (2)$$

where $K_d(z)$ is the diffuse attenuation coefficient estimated from Chl-a (Morel, 1988) as follows:

$$K_d(z) = 0.121\text{Chl–a}^{0.428}. \quad (3)$$

For this dataset, there was a strong linear relationship between surface and optically weighted Chl-a values (slope = 0.95, y intercept = 0.02, $r^2 = 0.98$), indicating that Chl-a$_{\text{weighted}}$ was rarely influenced by a deep chlorophyll-rich layer. Despite the similarity between surface Chl-a and Chl-a$_{\text{weighted}}$, the weighted Chl-a value was used in the match-up comparison because it more accurately reflects what a satellite sensor detects.

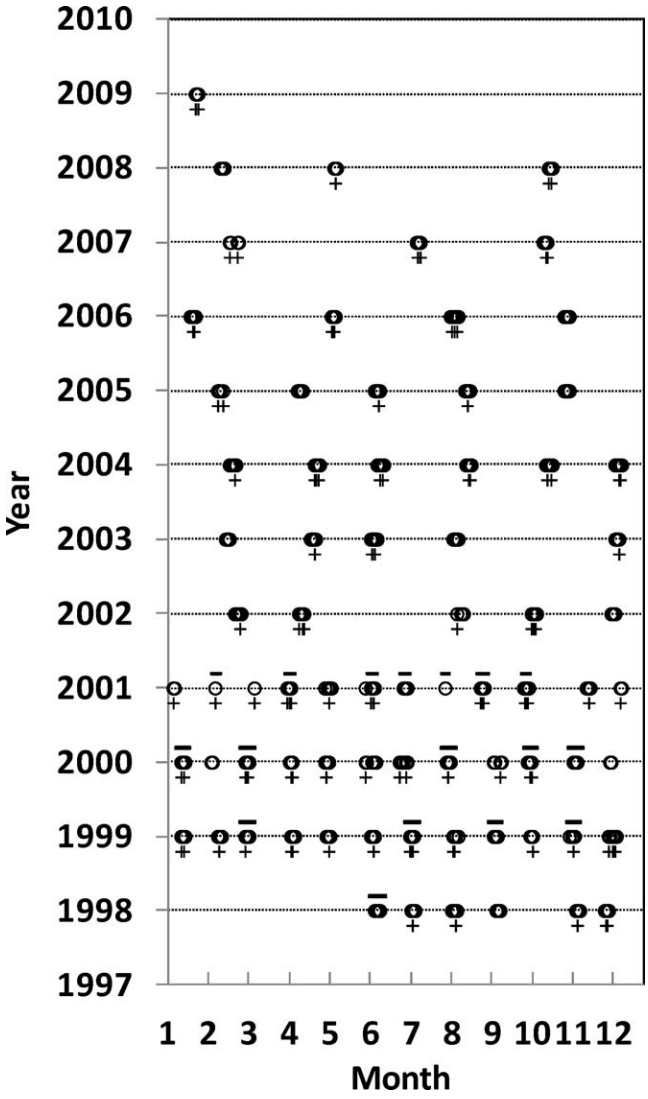

Figure 2. Temporal coverage of *in situ* remote sensing reflectance spectra (-), *in situ* Chl-a (○), and valid SeaWiFS Chl-a match-up data (+) for ECOHAB monthly (1998–2001) and South Florida Program bimonthly (2002–2009) cruises.

$R_{rs}(\lambda)$ spectra were also obtained during seventeen ECOHAB cruises (1998–2001; Figure 2). $R_{rs}(\lambda)$ was calculated from above-water spectral measurements of upwelling radiance, sky radiance, and the radiance from a standard diffuse reflector (Spectralon®; 10%) according the methods of Lee *et al.* (2010). Measurements were obtained using a custom-built 512-channel spectral radiometer (~350–850 nm; ~1.1 nm spectral resolution). $R_{rs}(\lambda)$ was then converted to $nL_w(\lambda)$ by multiplying

by the extraterrestrial solar irradiance ($F_0[\lambda]$) (Thuillier *et al.*, 2003) prior to validating SeaWiFS data. $nL_w(\lambda)$ was used rather than $R_{rs}(\lambda)$ so that results from this study can be compared to those reported previously during other global and regional validation efforts (Bailey and Werdell, 2006; Melin, Zibordi, and Berthon, 2007; Zibordi, Melin, and Berthon, 2006).

Satellite Data

SeaWiFS Level-2 data at approximately 1-km ground resolution were obtained from the NASA Goddard Space Flight Center. These data were generated from the at-sensor calibrated radiance (Level-1) using atmospheric correction and bio-optical inversion algorithms embedded in the software package SeaDAS (version 6.1). These algorithms represented the most recent progress in calibration updates and algorithm coefficient tuning using global data at the time of preparing this manuscript. The Level-2 data used in this study contained $nL_w(\lambda)$, Chl-a, and aerosol optical thickness at 865 nm ($\tau_a 865$). The data were projected to an equal-distance cylindrical projection in order to compare with *in situ* measurements.

Enhanced-RGB (ERGB) composite imagery was generated using SeaWiFS $nL_w(\lambda)$ data at 555 nm, 490 nm, and 443 nm. Such imagery was used in order to help determine why the SeaWiFS OC4 algorithm failed on several occasions: Dark features are caused by high absorption predominantly attributable to phytoplankton or CDOM and bright features are caused by either sediment resuspension or shallow bottom (Conmy *et al.*, 2009; Hu, 2008; Hu *et al.*, 2005).

Ancillary Data

Mean daily river discharge data (1998–2001) were obtained from the U.S. Geological Survey (USGS) for sites located along the Hillsborough (02304500), Alafia (02301500), Little Manatee (02300500), and Manatee (02299950) Rivers that empty into Tampa Bay and the Myakka (02298830), Peace (02296750), and Caloosahatchee (02292900) Rivers that empty into Charlotte Harbor (Figure 1). Hourly wind speed data (1998–2001) from the Coastal Marine Automated Network (C-MAN) station in Venice, Florida (VENF1; 27.070° N, 82.450° W) were downloaded from the NOAA National Data Buoy Center (http://www.ndbc.noaa.gov/).

Bio-optical Algorithm

SeaWiFS Chl-a was estimated using the standard OC4 algorithm (O'Reilly *et al.*, 2000) as follows:

$$\text{Chl–a} = 10.0^{(c_0+c_1R+c_2R^2+c_3R^3+c_4R^4)}, \quad (4)$$

where R is the $\log_{10}$ of the maximal remote sensing reflectance ratio: $R_{rs}(443)/R_{rs}(555) > R_{rs}(490)/R_{rs}(555) > R_{rs}(510)/R_{rs}(555)$. The constants ($c_0$-$c_4$) originally determined by O'Reilly *et al.* (2000) for a large, global data set have since been updated (http://oceancolor.gsfc.nasa.gov/REPROCESSING/R2009/ocv6/).

Match-up Criteria

For quality assurance, image pixels associated with any of the following quality flags were discarded: atmospheric correction failure or warning, sun glint, total radiance greater than knee value, large satellite or solar angle, cloud, stray light, low water-leaving radiance, and chlorophyll warning. These are the same flags used to discard low-quality data for global composites. For each *in situ* value (*i.e.* Chl-a or $nL_w[\lambda]$), the following criteria were used to find the "matching" SeaWiFS value: (1) SeaWiFS overpass within ±3 hours of *in situ* data collection; (2) more than half of the 3×3 SeaWiFS pixels centered at the *in situ* location showed valid data; and (3) coefficient of variation (standard deviation/mean) of $nL_w(443)$ from the valid pixels was less than 15%. This latter criterion was used to assure homogeneity within the 3×3 pixels so that satellite data (1-km resolution) and *in situ* data (point measurements) can be compared with each other. If all these criteria were met, then a matching pair between the mean of the valid SeaWiFS pixels and the *in situ* measurement was established.

Statistical Analysis

Both statistical and graphical criteria were used to assess the match-up comparisons between *in situ* and SeaWiFS estimates of Chl-a and $nL_w(\lambda)$. Because chlorophyll concentrations tend to be log-normally distributed in oceanic waters (Campbell, 1995), Chl-a values were logarithmically transformed before statistical analyses were performed.

Statistics used to assess the accuracy of satellite retrievals included the root mean square (RMS) error, calculated as

$$\text{RMS} = \sqrt{\frac{1}{N-2}\sum_{i=1}^{N}(x_i - y_i)^2}, \quad (5)$$

where x_i is the ith satellite-retrieved value, y_i is the ith *in situ* value, and N is the number of matching pairs. Median satellite-to-*in situ* ratios were determined to assess bias. Also, median absolute percent differences (APD) were calculated from the group $(|x_i - y_i|/y_i)_{i=1,N}$ to assess uncertainties. In terms of graphical criteria, linear regression (Type II-reduced major axis) slopes were determined to show how satellite and *in situ* values compare over the dynamic range. These bulk statistical and graphical measures were chosen because they have been reported previously for other validation studies, thus allowing results from this study to be directly compared to earlier results.

RESULTS

Accuracy of SeaWiFS $nL_w(\lambda)$

Prior to examining the accuracy of the OC4 Chl-a algorithm, comparisons were made between near-concurrent *in situ* and SeaWiFS $nL_w(\lambda)$ measured on the WFS during the ECOHAB field sampling program (1998–2001) (Figure 3, Table 1) to assess the accuracy of the atmospheric correction procedure for this region. Out of 245 available *in situ* $nL_w(\lambda)$ measurements made during this period, 91 valid match-up pairs (~37%) were found. *In situ* $nL_w(490)$ spanned almost an order of magnitude, ranging from 0.47 to 4.01 mW cm^{-2} μm^{-1} sr^{-1}, indicating that a wide range of environmental conditions were included in this validation data set. The median APD, used to assess uncertainty, was lowest at 510 nm (9.9%) with increasing uncertainty observed with decreasing wavelength. Median satellite to *in situ* ratios were within 3% of unity for blue-green wavelengths (412–555 nm), indicating low overall bias. Type

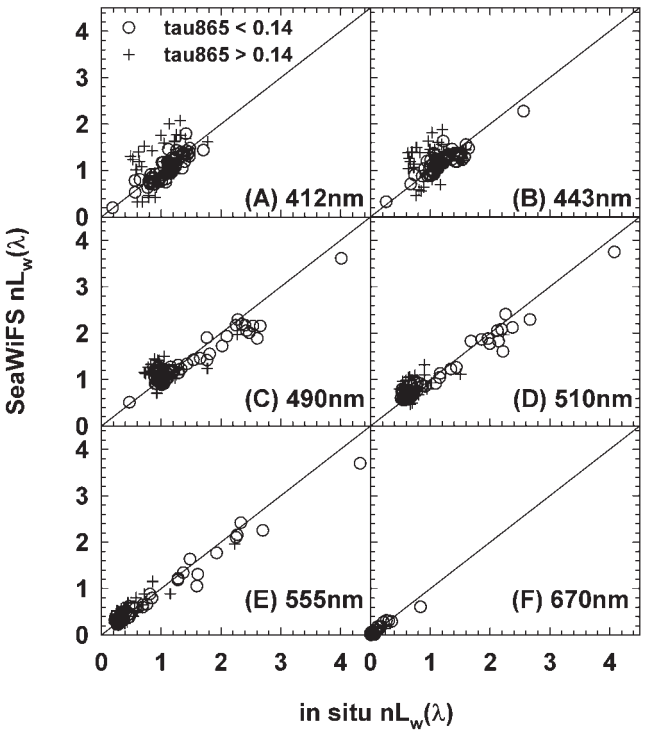

Figure 3. Scatterplots of SeaWiFS *vs. in situ* normalized water-leaving radiances, $nL_w(\lambda)$, at 412, 443, 490, 510, 555, and 670 nm (mW cm^{-2} μm^{-1} sr^{-1}) ($n = 91$) sorted by aerosol optical thickness: $\tau_a865 < 0.14$ (○) and $\tau_a865 > 0.14$ (+). *In situ* data were collected on the West Florida Shelf during the ECOHAB monthly cruises (1998–2001). The solid lines represent the 1:1 relationships.

II linear regression slopes in this spectral region ranged from 0.77 at 490 nm to 1.30 at 412 nm. Uncertainty (42.8%) and bias (11%) were higher at 670 nm because of the relatively lower values observed at this wavelength.

For $nL_w(412)$ and $nL_w(443)$, coefficients of determination ($r^2 < 0.34$) were less than half that observed for higher wavelengths. While this low correlation might partially be attributed to a smaller dynamic range in values, another explanation is atmospheric correction residual errors. Upon further investigation, the majority of outliers in Figure 3 were associated with elevated aerosol optical thicknesses (τ_a865) (Figure 4A), with the majority of overestimated satellite $nL_w(\lambda)$ collected on 28–29 August 2001 and underestimated values collected on 5 June 2001. Excluding match-up data with τ_a865 greater than 0.14 improved bulk statistical measures and linear regression results for all blue-green wavelengths (Table 1). Median APDs decreased (7–9%), and slope values were closer to unity (0.80–1.08). Improvements were greatest at 412 nm and 443 nm, with coefficients of determination doubling ($r^2 > 0.75$) and RMS errors halved after these data were excluded. These validation results indicate that the ability to accurately estimate satellite ocean color data products derived directly from $nL_w(\lambda)$ might be a challenge on the WFS under thick atmospheric aerosol conditions. Empirical Chl-a retrieval

Table 1. *Validation statistics for SeaWiFS normalized water-leaving radiances,* nL$_w$*(λ), at 412, 443, 490, 510, 555, and 670 nm for the West Florida Shelf (1998–2001). Statistics were calculated for all match-up data and for data with SeaWiFS aerosol optical thicknesses* ($\tau_a865 < 0.14$).

λ (nm)	τ_a865	N	Median Ratio	Median APD	Slope	r^2	RMS
412	all	91	0.97	13.7	1.296	0.344	0.315
	<0.14	65	0.95	8.2	1.079	0.750	0.148
443	all	91	1.01	10.3	0.967	0.323	0.288
	<0.14	65	0.99	7.0	0.840	0.775	0.141
490	all	91	1.01	10.1	0.771	0.829	0.256
	<0.14	65	1.00	7.5	0.802	0.940	0.197
510	all	91	1.03	9.9	0.857	0.914	0.199
	<0.14	65	1.01	6.6	0.877	0.970	0.145
555	all	91	1.00	12.7	0.853	0.957	0.160
	<0.14	65	0.98	8.6	0.881	0.979	0.141
670	all	91	1.11	42.8	0.779	0.826	0.044
	<0.14	65	1.01	28.7	0.828	0.926	0.037

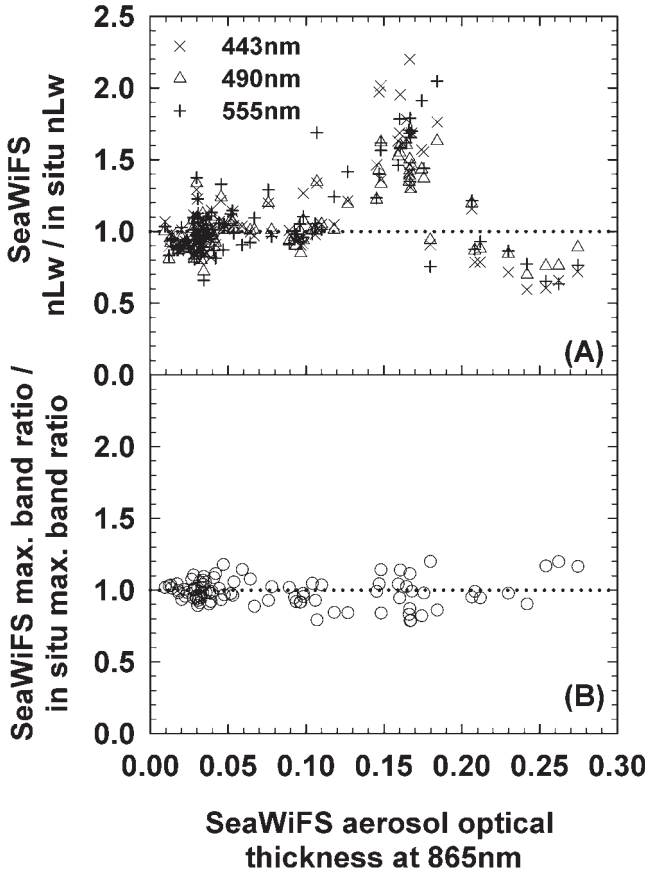

Figure 4. Ratios of SeaWiFS-to-*in situ* (A) normalized water-leaving radiances at 443 nm (×), 490 nm (Δ), and 555 nm (+) and (B) maximum OC4 band-ratios; *e.g.* greater of $nL_w(443)/nL_w(555)$, $nL_w(490)/nL_w(555)$, and $nL_w(510)/nL_w(555)$ (○), both plotted as a function of the SeaWiFS aerosol optical thickness (τ_a865). *In situ* data were collected on the West Florida Shelf during the ECOHAB monthly cruises (1998–2001). The horizontal dotted lines represent perfect agreement between satellite and *in situ* values.

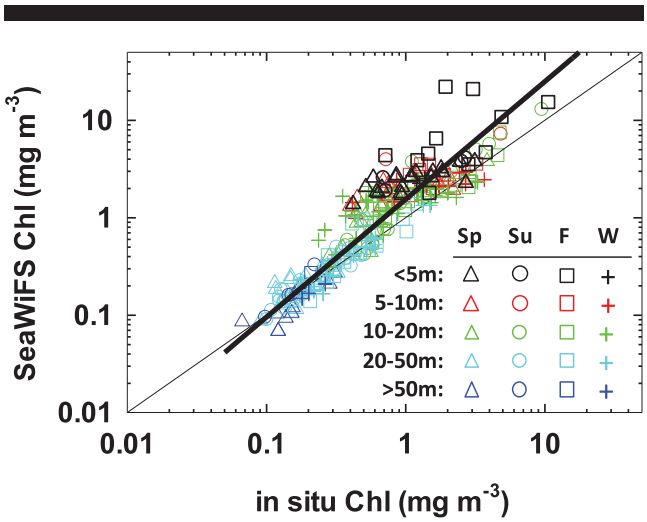

Figure 5. Scatterplot of near-concurrent SeaWiFS and *in situ* Chl-a concentrations (mg m^{-3}) for the WFS (1998–2009). SeaWiFS Chl-a was estimated using the globally tuned OC4 algorithm. Match-up data were sorted seasonally (Spring—21 March to 20 June; Summer—21 June to 22 September; Fall—23 September to 20 December; Winter—21 December to 20 March) and spatially by bottom depth (<5 m, 5–10 m, 10–20 m, 20–50 m, and >50 m). The thin solid line represents the 1 : 1 relationship. The thick solid line represents the best-fit linear regression relationship (slope = 1.21, *y* intercept = 0.19, $r^2 = 0.844$, $n = 289$).

algorithms such as the OC4 band-ratio algorithm, however, are less sensitive to absolute errors in $nL_w(\lambda)$, as these errors partially cancel out with maximal band ratios exhibiting reduced uncertainty (median APD = 5%) (Figure 4B).

Indeed, it is never possible to validate satellite measurements at all locations for a prolonged period using *in situ* measurements. On the other hand, data-quality statistics can be generated from satellite data alone, which can provide useful information on the spatiotemporal distributions of data quality. Examination of the SeaWiFS data for the entire mission (1997–2010) showed that SeaWiFS $\tau_a 865$ was >0.14 only <10% of the time. Thus, for most of the time $nL_w(\lambda)$ should be regarded as valid, especially for nL_w ratios; however, occasionally negative $nL_w(412)$ did occur because of atmospheric correction errors. The occurrence is mostly restricted to nearshore waters (<10-m isobath) with frequency ranging between 5% to 20%. More negative $nL_w(412)$ occurred in summer and fall (~10–20%) than in winter and spring (~5–10%), attributable to increased coastal runoff during the south-central Florida wet season and the tendency for HABs to occur at this time of the year. Both CDOM and phytoplankton blooms can lead to decreasing *in situ* $nL_w(412)$ and increasing likelihood of negative satellite $nL_w(412)$ (*i.e.* when *in situ* $nL_w(412)$ is low, a slight atmospheric correction error may lead to negative $nL_w[412]$). Even if $nL_w(412)$ is negative, however, nL_w in other bands, especially at 490–555 nm, which are used in the OC4 band-ratio algorithm for the coastal waters of the WFS, are typically still valid for Chl-a retrievals. In contrast, these negative $nL_w(412)$ errors may cause significant algorithm artifacts for semianalytical algorithms that are heavily dependent on $nL_w(412–443)$.

Table 2. *Validation statistics for SeaWiFS Chl-a concentrations derived using the default OC4 algorithm for the West Florida Shelf (1998–2009). Statistics were calculated for the entire data set and for various data subsets based on water column depth.*

Water Depth (m)	*N*	Median Ratio	Median APD	Slope	r^2	RMS
> 0	289	1.25	29.6	1.21	0.844	0.256
> 5	249	1.16	24.1	1.15	0.863	0.213
>10	211	1.12	19.8	1.13	0.879	0.183
>20	123	1.01	14.0	1.09	0.891	0.107
>30	92	0.99	13.2	1.08	0.833	0.108
>50	35	0.93	12.2	1.23	0.817	0.108

Accuracy of SeaWiFS OC4 Chl-a

SeaWiFS OC4 Chl-a were compared to near-concurrent *in situ* values in order to determine how well this globally tuned algorithm performed on the WFS (Figure 5). Out of 2888 available *in situ* Chl-a measurements from both the ECOHAB and SFP field campaigns (1998–2009), 289 valid match-up pairs (~10%) were found. These match-up data were sorted by bottom depth, which was used as a proxy for distance offshore (*e.g.* degree of terrestrial and bottom influence) and by season in order to examine how the level of agreement between satellite and *in situ* Chl-a changed both spatially and temporally, respectively. In this study, seasons were demarcated based on dates of the Northern Hemisphere equinoxes and solstices and were defined as follows: Spring (21 March–20 June), Summer (21 June–22 September), Fall (23 September–20 December), and Winter (21 December–20 March). Statistical results of this match-up comparison are provided in Table 2.

In situ and SeaWiFS Chl-a spanned more than two orders of magnitude and ranged from 0.07 to 10.6 mg m^{-3} and 0.07 to 20.2 mg m^{-3}, respectively, indicating that a wide range of trophic levels were represented by this validation data set (Figure 5). Overall, *in situ* and SeaWiFS Chl-a were highly correlated ($r^2 = 0.84$, $n = 289$); however, satellite values were positively biased with a median satellite-to-*in situ* Chl-a ratio of 1.25 (Table 2). While SeaWiFS Chl-a below ~0.5 mg m^{-3} agreed well with *in situ* values, values greater than ~0.5 mg m^{-3} were often overestimated by up to a factor greater than 10. No temporal trend in algorithm performance was observed based on examination of Figure 5, with overestimations occurring during all seasons. Algorithm performance degraded steadily, though, with decreasing water column depth (*i.e.* increased proximity to shore). When match-up data shoreward of the 20-m isobath were excluded, the median ratio (1.01) and linear regression values (slope = 1.09, $r^2 = 0.89$) were much closer to unity. In addition, the median APD (14.0%) and RMS error (0.107) for this data subset were less than half those determined when all match-up data were considered. Algorithm performance continued to improve with increasing distance offshore as validation data in shallower waters were gradually excluded. This improvement appeared to decline when only stations located offshore of the 50-m isobath were considered. Rather than indicating a decline in algorithm performance, though, this was likely a result of the smaller dynamic range and size of this data subset.

Figures 6 and 7 show Hovmöller diagrams of *in situ* and SeaWiFS OC4 Chl-a for an along-shelf (10-m isobath) and

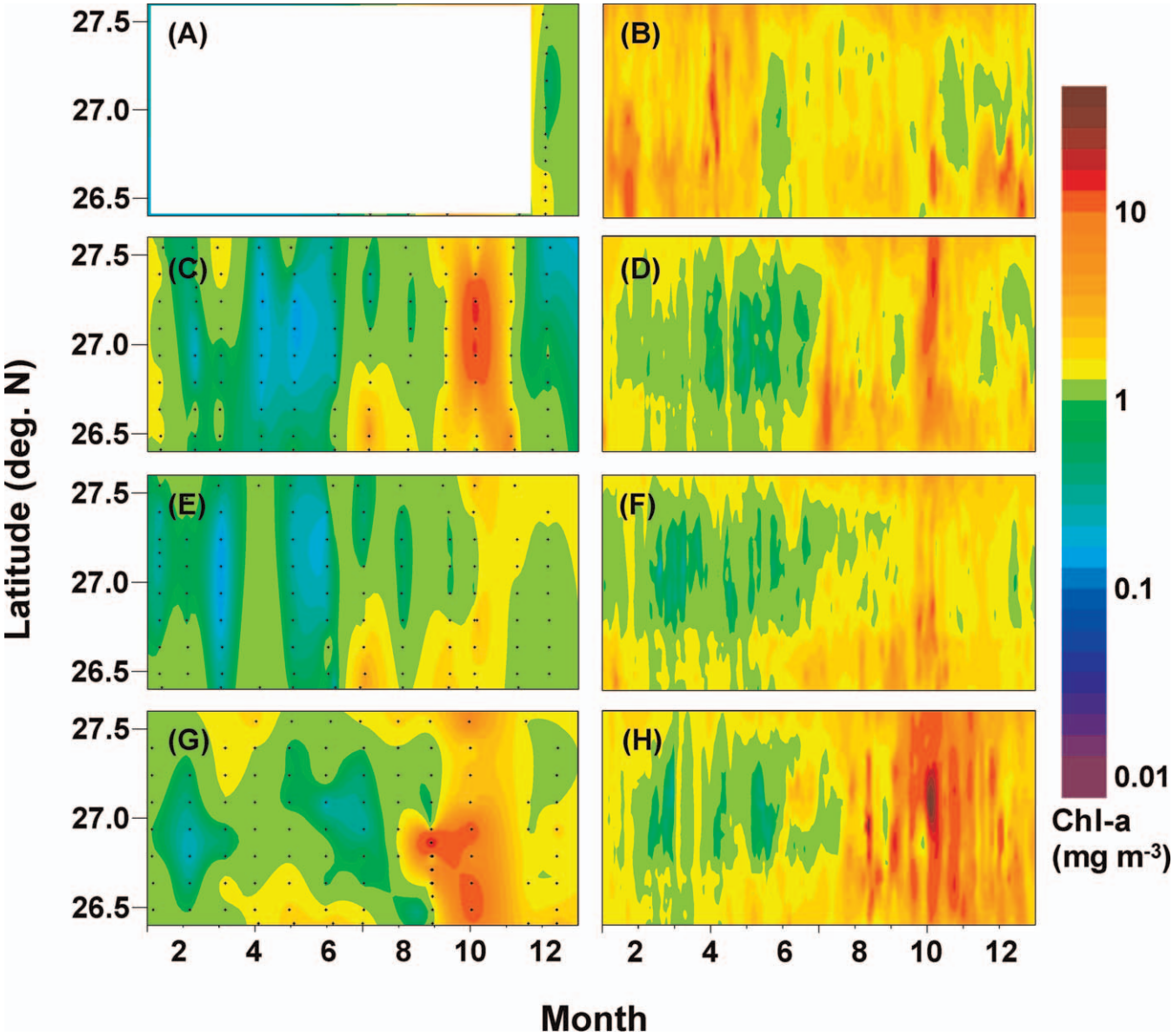

Figure 6. Hovmöller diagram of *in situ* (left column) and SeaWiFS (right column) Chl-*a* concentrations (mg m^{-3}) for an along-shelf transect located between Charlotte Harbor and Tampa Bay on the 10-m isobath in (A, B) 1998, (C, D) 1999, (E, F) 2000, and (G, H) 2001. SeaWiFS data were extracted daily every 5 km along this transect. Note that *in situ* data were not collected along this transect prior to December 1998. See Figure 1 for transect location.

cross-shelf (~10–50-m isobaths) transect, respectively (Figure 1). Both transects were sampled monthly during the ECOHAB program (1998–2001) except for during poor weather conditions. Overall, the general patterns observed between *in situ* and satellite-derived Chl-a matched along both transects with the lowest values (<0.2 mg m^{-3}) occurring during the summer in offshore waters and during late-winter/spring in nearshore waters away from areas influenced heavily by estuarine discharge. In contrast, the highest Chl-a values (>10 mg m^{-3}) were observed mainly in nearshore waters during south-central Florida's wet season in late-summer/fall and when nearshore blooms of mixed diatoms (*e.g.* July 1999 and July 2000) and HABs of ichthyotoxic *Karenia brevis* (*e.g.* November–December 1998, October 1999, October–November 2000, and August–December 2001) were observed.

While relative patterns from the two observations matched well, the absolute values differed significantly, particularly for the along-shelf transect where Chl-a was typically >0.5 mg m^{-3} (Figure 6). Here, SeaWiFS Chl-a was significantly higher than *in situ* Chl-a, especially at the northern and southern ends of the transect where discharge from the many rivers flowing into

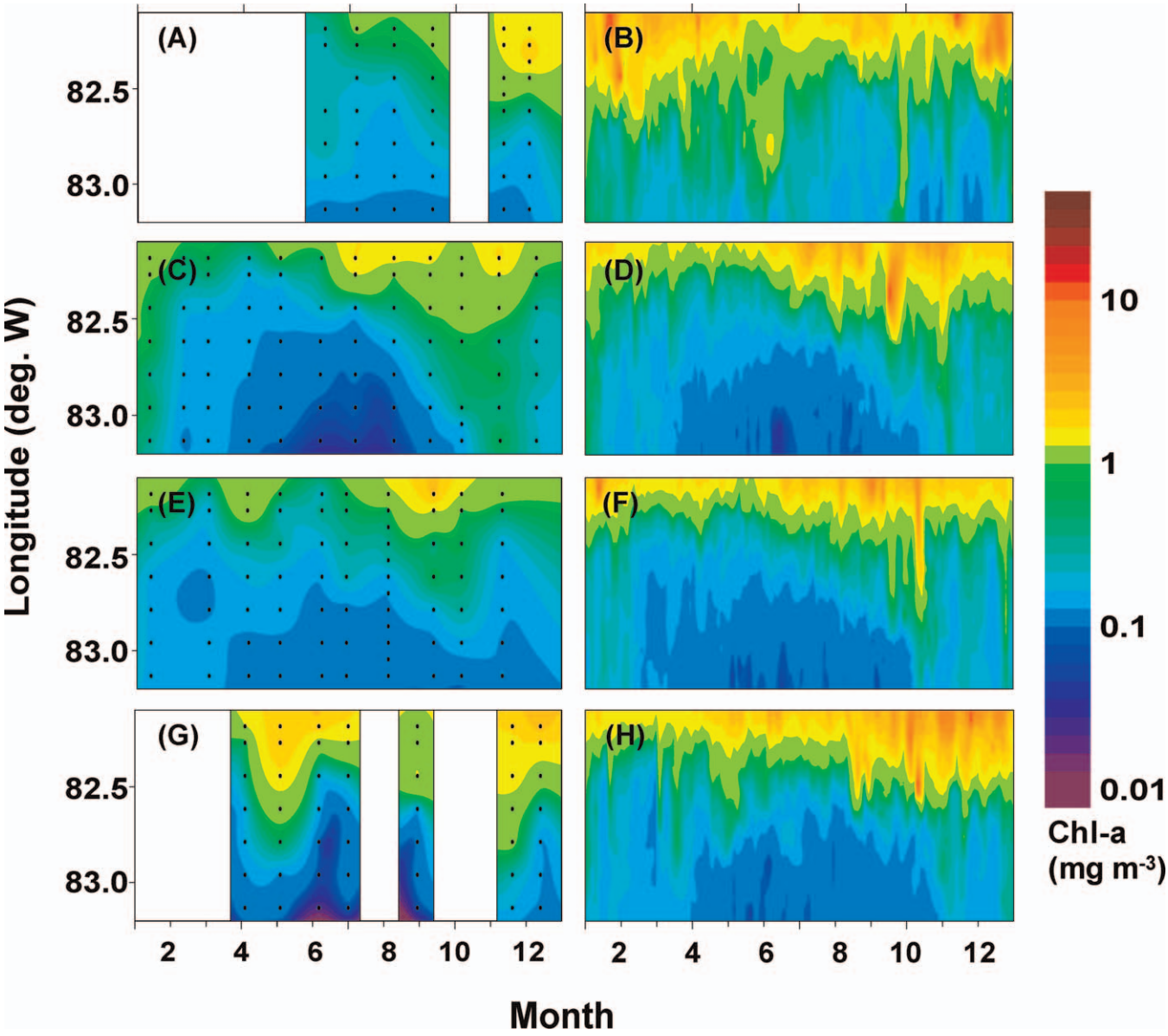

Figure 7. Hovmöller diagram of *in situ* (left column) and SeaWiFS (right column) Chl-a concentrations (mg m^{-3}) for a cross-shelf transect located offshore of the Caloosahatchee River between the 10- and 50-m isobaths in (A, B) 1998, (C, D) 1999, (E, F) 2000, and (G, H) 2001. SeaWiFS data were extracted daily every 5 km along this transect. Note that *in situ* data were not collected along this transect prior to June 1998 and when poor weather conditions prevented shipboard surveys from being conducted in offshore waters. See Figure 1 for transect location.

Tampa Bay and Charlotte Harbor were greatest and also during the wet season in general.

Sources of Error

The tendency for SeaWiFS Chl-a to be overestimated in nearshore waters was also observed in a 4-year time series (January 1998–December 2001) at ECOHAB Station 78 (27.089° N, 82.546° W; Figure 8), located midway between Tampa Bay and Charlotte Harbor on the 10-m isobath (Figure 1). Again, while the overall temporal trends in both time series were similar, with lower values typically observed in winter–spring during the dry season and higher values observed in summer–fall during the wet season and when both harmful and non-harmful algal blooms tended to occur, SeaWiFS Chl-a was consistently overestimated. In order to examine the underlying reasons for these overestimations, match-up data at (or near) this station were examined on four occasions. These four case studies included periods of (1) high discharge (6 April 1998), (2) HAB (19 November 2001), (3) wind-driven sediment resuspension (5 January 2001), and (4) calm weather with low discharge (3 March 2000) (Table 3).

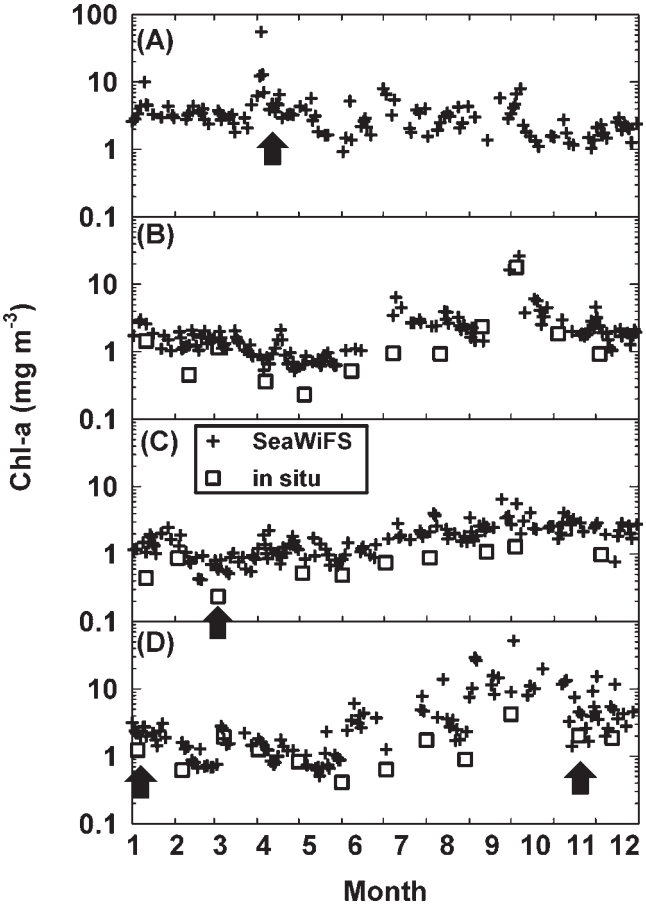

Figure 8. *In situ* (□) and SeaWiFS (+) Chl-a concentrations (mg m^{-3}) observed at ECOHAB Station 78 (27.089° N, 82.546° W) in (A) 1998, (B) 1999, (C) 2000, and (D) 2001. Arrows indicate the four case studies chosen for further examination when SeaWiFS OC4 Chl-a was overestimated at (or near) station 78 on 6 April 1998, 3 March 2000, 5 January 2001, and 19 November 2001. See Figure 1 for station location.

CDOM

Mean daily discharge for the seven major rivers that flow into Tampa Bay (Hillsborough, Alafia, Little Manatee, and Manatee) and Charlotte Harbor (Myakka, Peace, and Caloosahatchee) were relatively high during summer and fall between January 1998 and December 2001, as is typical during south-central Florida's wet season (Figure 9). Discharge in winter and spring was generally low except for during the 1997–98 El Niño event when south-central Florida experienced significantly higher rainfall and discharge (Schmidt *et al*., 2001). The median SeaWiFS Chl-a at Station 78 during the spring of 1998 was ~3–4 times higher than that measured during the following three non-El Niño years (Figure 8). Was this a realistic increase (*e.g*. attributable to algal growth stimulated by excess nutrients) or an algorithm artifact attributable to excess terrestrial CDOM associated with the heavy discharge?

Mean discharge in west-central Florida peaked that year on 22 March (Figure 9). Two weeks later, SeaWiFS Chl-a at Station 78 also peaked and then decreased from 55.8 mg m^{-3} to 5.50 mg m^{-3} by 6 April (Figure 8). Shipboard Chl-a and spectral absorption data for CDOM ($a_{CDOM}[\lambda]$), phytoplankton ($a_{ph}[\lambda]$), and detritus (nonalgal particles) ($a_d[\lambda]$) were measured ~36 hours later on 8 April by the University of South Florida just 10 km NW of Station 78 at 27.167° N and 82.598° W. SeaWiFS Chl-a (6.50 mg m^{-3}) determined at this nearby site was ~287% higher than the *in situ* value (1.68 mg m^{-3}) (Table 3).

SeaWiFS ERGB composite imagery collected on 6 April (Figure 10A) showed both stations in the same dark-reddish patch of water observed between Tampa Bay and Charlotte Harbor that extended out to the 20-m isobath. SeaWiFS $R_{rs}(\lambda)$ at both sites were similar, exhibiting relatively low $R_{rs}(\lambda)$ between 412 nm and 670 nm (<0.004 sr^{-1}), indicating high absorption. *In situ* data collected at the station 10 km NW of Station 78 showed $a_{CDOM}(440) = 0.37\ m^{-1}$, $a_{ph}(440) = 0.08\ m^{-1}$, and $a_d(440) = 0.02\ m^{-1}$, confirming the CDOM dominance of both absorption and reflectance at 440 nm and explaining the overestimation in SeaWiFS Chl-a. Given the high discharge observed during the entire winter–spring of 1998 (Figure 9) as well as the corresponding high-CDOM and low-salinity waters on the shelf (Nababan, 2005), it is likely that SeaWiFS Chl-a was overestimated in nearshore waters, which was influenced by terrestrial outflow during this time (Figures 6 and 7); however, adding to this complexity is nutrient-rich coastal upwelling that also occurred during this time, possibly fueling phytoplankton growth in nearshore waters (Weisberg *et al*., 2004).

HABs

During the ECOHAB field sampling program (1998–2001), four major HABs of *K. brevis* were observed on the central

Table 3. *Four case studies examined when SeaWiFS Chl-a determined using the globally tuned OC4 algorithm was overestimated at (or near) ECOHAB station 78 (27.089° N, 82.546° W) located between Tampa Bay and Charlotte Harbor on the 10-m isobath.*

Date	*In situ* Chl-a (mg m^{-3})	SeaWiFS OC4 Chl-a (mg m^{-3})	SeaWiFS ERGB Imagery	Wind Speed	River Discharge	Factor Responsible for Overestimation
6 April 1998	- (1.68)[a]	5.50 (6.50)[a]	dark; reddish brown	low	high	CDOM
19 November 2001	2.05	4.56	dark; reddish brown	-	-	harmful algal bloom
5 January 2001	1.24	2.03	white	high	low	suspended sediments
3 March 2000	0.24	0.59	white/cyan; sand bars visible	low	low	bottom reflectance

[a] Data in parenthesis were obtained 10 km NW of ECOHAB station 78 at 27.167° N, 82.598° W. *In situ* data were collected on 8 April 1998, and SeaWiFS data were collected ~36 hours earlier on 6 April 1998.

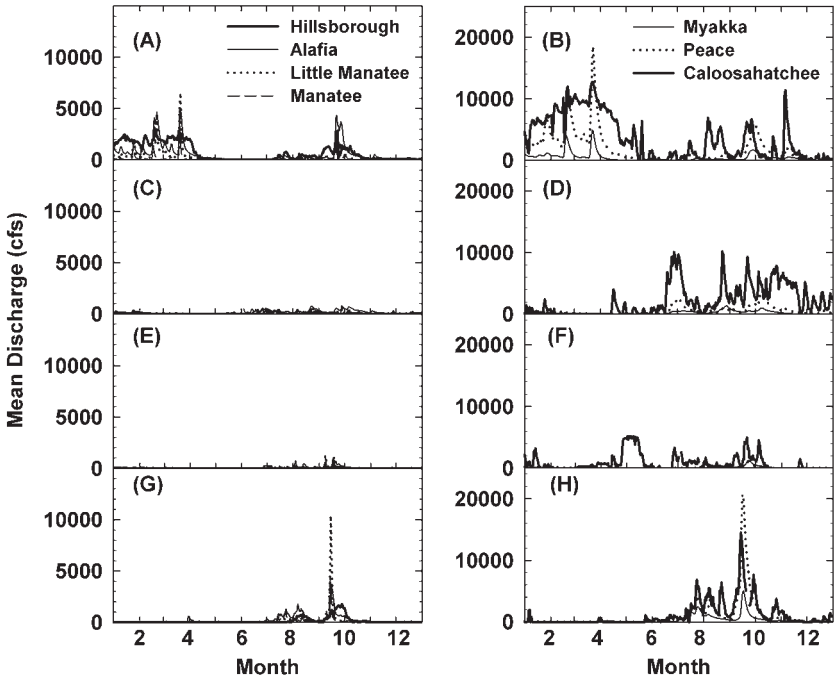

Figure 9. Mean daily discharge (cu ft sec^{-1}) for the Hillsborough, Alafia, Little Manatee, and Manatee Rivers (left column) and the Myakka, Peace, and Caloosahatchee rivers (right column) in (A, B) 1998, (C, D) 1999, (E, F) 2000, and (G, H) 2001. River locations are shown in Figure 1.

WFS, exhibiting variable magnitudes ($\sim 10^3$–10^6 cells l^{-1}), durations (2–10 months), and areal extents ($\sim$700-7000 km^2) (Vargo *et al*., 2008). Of these four blooms, two were observed at Station 78 during October 1999 and September–December 2001. On both occasions, SeaWiFS Chl-a exceeded 25 mg m^{-3} (Figure 8). While SeaWiFS Chl-a agreed with *in situ* measurements during the October 1999 bloom, satellite Chl-a was often higher than *in situ* values during the late 2001 bloom.

This latter bloom first appeared in surface waters in late August just north of Charlotte Harbor and was later transported northward to Tampa Bay (Cannizzaro *et al*., 2008; Vargo *et al*., 2008). On 19 November, SeaWiFS Chl-a (4.56 mg m^{-3}) at Station 78 was 122% higher than the *in situ* Chl-a (2.05 mg m^{-3}) obtained within 10 hours of the satellite measurement (Table 3). SeaWiFS ERGB imagery (Figure 10C) indicated the presence of a large dark-reddish patch of water extending from Tampa Bay southward to Charlotte Harbor and offshore to the $\sim$20–30 m isobaths. SeaWiFS $R_{rs}(\lambda)$ values between 412 and 670 nm at Station 78 were relatively low ($<$0.004 sr^{-1}), indicating high absorption primarily attributable to the high concentration of *K. brevis* (342,000 cells l^{-1}) and possibly high CDOM absorption given that mean daily discharge for the Caloosahatchee River observed the month prior was moderately high ($\sim$20–4000 cu ft s^{-1}; Figure 9H). Differences observed between *in situ* and SeaWiFS Chl-a on this occasion might also be explained by a lack of spatial homogeneity in cell concentrations both vertically and horizontally (Franks, 1997; Subramaniam *et al*., 2002) and by the unique optical properties exhibited by *K. brevis* blooms (Cannizzaro *et al*., 2008).

Suspended Sediments

SeaWiFS Chl-a (2.03 mg m^{-3}) at Station 78 was also overestimated (by 64%) immediately following a winter storm event on 5 January 2001 (Figure 8, Table 3). Data recorded at a C-MAN station located in Venice, Florida, showed a strong winter frontal system passed across the state of Florida 1 week prior to this date, with maximal wind speeds of 13 m s^{-1}. SeaWiFS ERGB imagery indicated the presence of highly reflective as opposed to dark (*e.g*. absorption-rich) waters along the entire west coast of Florida extending out to the 20-m isobath (Figure 10E). SeaWiFS $R_{rs}(\lambda)$ measured at all wavebands between 412 and 670 nm at Station 78 on 5 January was relatively high ($\sim$0.005–0.030 sr^{-1}) and was attributed to enhanced backscattering caused by storm-related sediment resuspension. Figure 11 shows a 4-year time series (1998–2001) of SeaWiFS $R_{rs}(670)$ measured at Station 78, which can be used as a proxy for suspended sediment concentrations (Stumpf and Pennock, 1989). A sharp increase in SeaWiFS $R_{rs}(670)$ ($>$0.02 sr^{-1}) occurred on 31 December 2000 immediately following the passage of this storm, followed by sustained $R_{rs}(670)$ values of $>$0.005 sr^{-1} for more than a week, causing overestimation of in SeaWiFS Chl-a.

Although SeaWiFS $R_{rs}(670)$ is not available every day mainly attributable to cloud cover, relative patterns of sediment resuspension events could still be inferred from Figure 11. SeaWiFS $R_{rs}(670)$ at Station 78 increased to $>$0.003 sr^{-1} within a short period of time on 36 separate occasions ($\sim$6–11 events

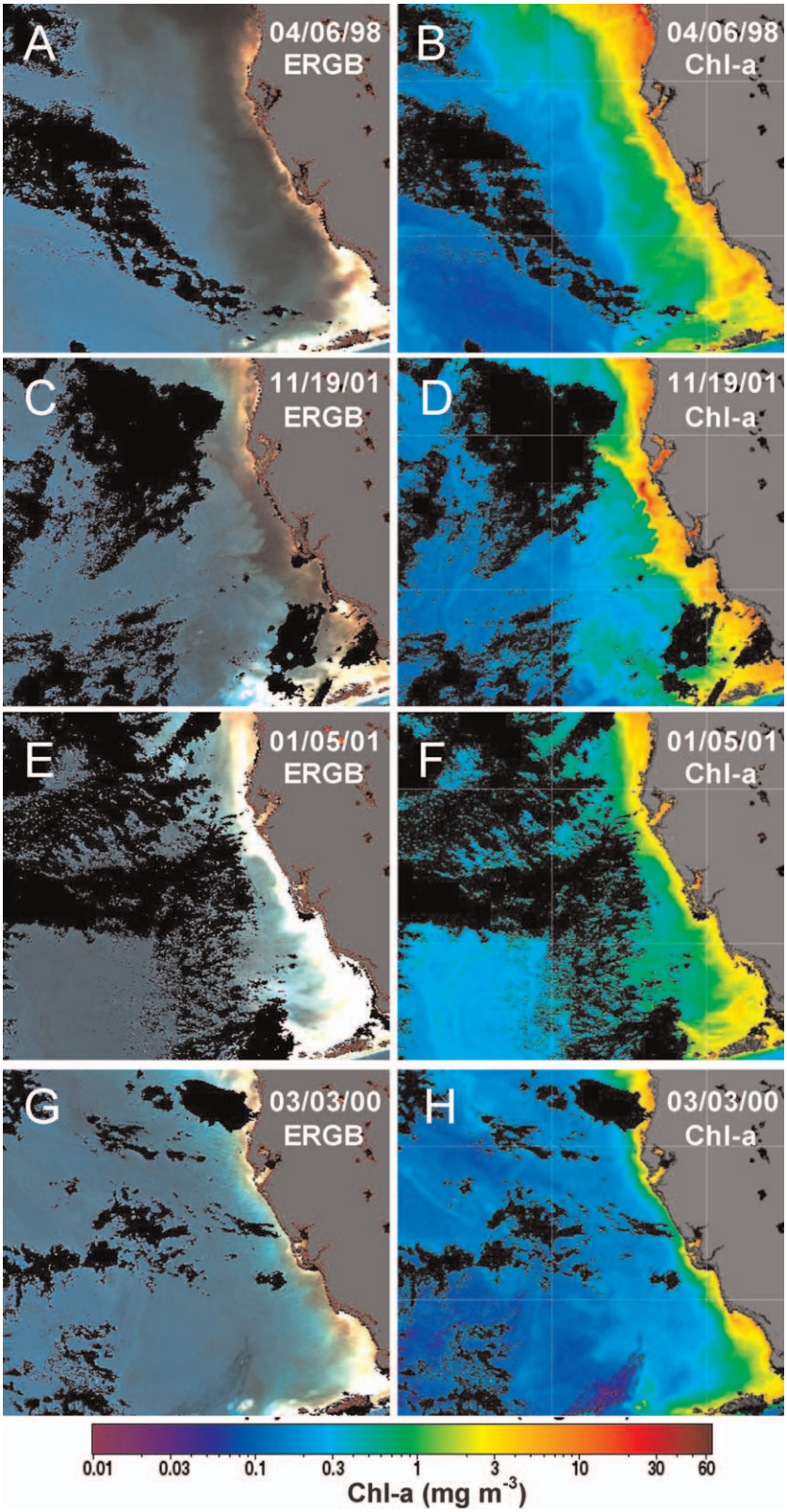

Figure 10. SeaWiFS enhanced-RGB (ERGB) composite imagery (left column) and Chl-a concentrations (mg m^{-3}) (right column) for 6 April 1998 (A, B), 19 November 2001 (C, D), 5 January 2001 (E, F), and 3 March 2000 (G, H). SeaWiFS Chl-a was estimated using the default OC4 algorithm.

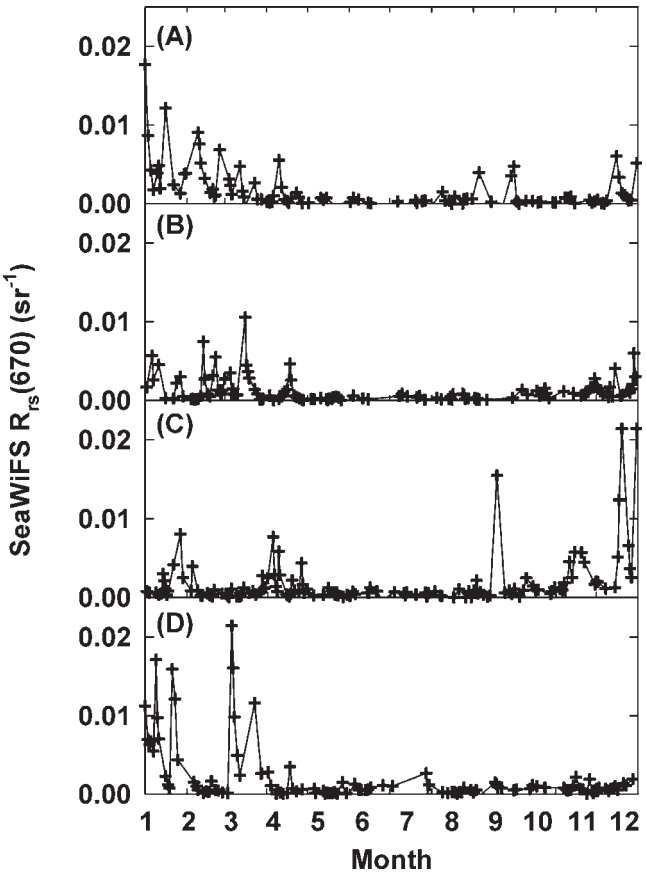

Figure 11. Temporal variability of SeaWiFS R_{rs}(670) (sr^{-1}) (+) observed at ECOHAB Station 78 (27.089° N, 82.546° W) in (A) 1998, (B) 1999, (C) 2000, and (D) 2001.

per year). Wind speed data recorded by the C-MAN station in Venice indicated that each of these periods of increased R_{rs}(670) was preceded by short-term wind events within the previous few days, with wind speeds exceeding 6 m s^{-1}. The majority of these wind events were associated with frontal passages that occurred during winter and early spring. From late spring to early fall, sediment resuspension events caused by increased wind activity were rare except for when highly energetic tropical storms (*e.g.* Hurricane Gordon—18 September 2000) passed through the region.

Bottom Reflectance

After winter-spring frontal activity subsided (as depicted by a decrease in SeaWiFS R_{rs}[670] in Figure 11) and before the beginning of the traditional wet season when terrestrial discharge associated with CDOM loading increased (Figure 9), *in situ* Chl-a at Station 78 during late winter and spring was relatively low (<0.5 mg m^{-3}; Figure 8), with the lowest (0.24 mg m^{-3}) being measured on 3 March 2000. SeaWiFS Chl-a (0.59 mg m^{-3}) observed at that location within 3 hours of the shipboard measurement was 146% higher than the *in situ* value (Table 3). Mean discharge rates for west-central Florida rivers measured up to a month prior to this date were low (<220 cu ft s^{-1}; Figure 9), indicating that high CDOM absorption was not responsible for causing this overestimation in Chl-a. Also, wind speeds (<5 m s^{-1}) recorded by the C-MAN station in Venice and SeaWiFS R_{rs}(670) data (<0.0005 sr^{-1}) (Figure 11) measured up to 3 days before this date were also relatively low, indicating no recent sediment resuspension event. SeaWiFS ERGB imagery (Figure 10G) further showed that the waters at Station 78 were neither dark (attributable to high CDOM and/or phytoplankton absorption, *e.g.* Figures 10A and C) nor bright (attributable to high suspended sediment concentrations, *e.g.* Figure 10E). Instead, the white/cyan colors along the central WFS together with the presence of visible sand bars indicated contribution of bottom reflection to $R_{rs}(\lambda)$ (Hu, 2008).

Hyperspectral shipboard $R_{rs}(\lambda)$ measured at Station 78 that day (3 March 2000) was inverted using the Lee *et al.* (1999) $R_{rs}(\lambda)$ optimization technique to determine relative reflectance contributions from the water column and the bottom. Results indicated that more than half of the light reflected at 490, 510, and 555 nm originated from the bottom. This bottom-related R_{rs} contribution would lead to lower blue-to-green reflectance band ratios, which, in turn, would lead to higher satellite-derived OC4 Chl-a than from a deep ocean.

DISCUSSION

Validation results are presented in this study for both SeaWiFS $nL_w(\lambda)$ and Chl-a using shipboard data collected regularly on the WFS for over a decade (1998–2009). These data were collected from a wide range of environments, including optically complex coastal waters influenced by riverine discharge, HABs, wind-driven sediment resuspension, or bottom reflectance to offshore, oligotrophic waters devoid of terrestrial discharge, blooms, and bottom effects. The RMS uncertainty for SeaWiFS Chl-a on the WFS estimated using the standard OC4 algorithm was 0.255 when all match-up data were considered. Similar errors were obtained during previous validation efforts in other coastal regions including the Northern Adriatic Sea (0.27) (Melin, Zibordi, and Berthon, 2007) and Patagonian Continental Shelf (0.23) (Dogliotti *et al.*, 2009). Omitting match-up data collected near shore of the 20-m isobath on the WFS yielded a reduced level of RMS uncertainty (0.106), indicating that the OC4 algorithm performs adequately in these less optically complex waters.

Although the positive bias observed in the default SeaWiFS OC4 Chl-a data product in nearshore waters has been reported previously for the Eastern Gulf of Mexico (Hu *et al.*, 2003b; Nababan, 2010; Schaeffer *et al.*, 2012; Stumpf *et al.*, 2000), this is the first time the various reasons for these overestimations are explicitly explained with potential occurrence frequencies determined in both space and time. Results here show that while this bias occasionally may be attributed to atmospheric correction errors, the accurate SeaWiFS $nL_w(\lambda)$ data for >90% time of the year, especially for the 490–555 nm wavelength range, suggest that most of the bias is a result of the Chl-a inversion algorithm.

Several tools were used in this study to evaluate where, when, and why the SeaWiFS Chl-a algorithm performed poorly,

with examples shown for four case studies (Table 3). SeaWiFS ERGB imagery helped differentiate between dark (*e.g.* absorption-rich) water masses influenced strongly by CDOM and/or phytoplankton blooms from bright (*e.g.* reflectance-rich) water masses influenced significantly by bottom reflectance or suspended sediments (Conmy *et al.*, 2009; Hu *et al.*, 2005). Ancillary wind speed and SeaWiFS $R_{rs}(670)$ data helped further determine whether bright areas observed in SeaWiFS ERGB imagery were attributable to bottom reflectance or resuspended sediments after a recent storm event.

The source of dark features in SeaWiFS ERGB imagery are more difficult to identify because CDOM and phytoplankton both absorb blue light strongly, resulting in decreased reflectance for blue-green wavebands. Hu *et al.* (2008) demonstrated that *K. brevis* blooms and coastal river plumes showed statistically similar $R_{rs}(\lambda)$ in this spectral region. Similar results were observed during this study for a *K. brevis* bloom (November 2001) and a CDOM plume associated with the 1997–98 El Niño event (April 1998), where SeaWiFS $R_{rs}(\lambda)$ at 412–670 nm were <0.004 sr^{-1}. While river discharge data can help determine when terrestrial outflow might be introducing high amounts of CDOM to shelf waters thus impacting the accuracy of satellite-derived Chl-a, *K. brevis* HABs have been known to occur at or near frontal regions associated with freshwater CDOM plumes attributable to physical forcing and light requirements (Vargo *et al.*, 2008; Walsh *et al.*, 2006). Consequently, alternative wavebands are required to differentiate between highly absorbing CDOM-rich waters and algal blooms. Hu *et al.* (2005) showed that the MODIS fluorescence line height data product, also available for MERIS, can help discriminate between these two OSCs, yet the lack of fluorescence bands makes this approach inapplicable for SeaWiFS.

Two approaches have commonly been employed for adapting the SeaWiFS OC4 Chl-a algorithm to perform optimally for various coastal regions. The first approach is to empirically correct satellite-derived values, as was performed for Massachusetts Bay (Hyde, O'Reilly, and Oviatt, 2007), Chesapeake Bay (Werdell *et al.*, 2009), and Florida coastal waters (Schaeffer *et al.*, 2012). Although this approach works well in eutrophic waters that exhibit a relatively small Chl-a dynamic range, Chl-a on the WFS spans more than two orders of magnitude, creating artifacts in individual images when the empirical adjustment is only applied to a portion of the image *(e.g.* Denman and Abbott,1988). The second approach is to locally tune the existing SeaWiFS OC4 algorithm coefficients (Werdell *et al.*, 2009). While this approach may provide a smooth (*i.e.* artifact-free) transition in Chl-a between oligotrophic, offshore, and eutrophic, nearshore waters, effectively reducing the overall bias observed with the default algorithm, though it would fail to capture any more of the actual dynamic variation in Chl-a than the unmodified OC4 algorithm. Likewise, an anomaly method may partially remove the Chl-a overestimation when performing time-series analysis or detecting new blooms (*e.g.* Stumpf *et al.*, 2003b), yet the data scattering shown in Figure 5 indicates that the positively biased Chl-a estimation would still result in residual errors.

Clearly, a more sophisticated approach for estimating satellite-derived Chl-a in nearshore waters (<20 m) of the WFS is required that takes into consideration all the various factors (*e.g.* CDOM, HABs, resuspended sediments, and bottom reflectance) that negatively impact the default OC4 algorithm. Future approaches may incorporate alternative wavebands located in spectral regions less influenced by CDOM and bottom contributions (Dall'Olmo *et al.*, 2005; Hu *et al.*, 2005; Le *et al.*, 2013a,b). They may also include look-up table (Gohin, Druon, and Lampert, 2002), semianalytical (Carder *et al.*, 1999; Lee *et al.*, 1999; Lee, Carder, and Arnone, 2002; Lyon *et al.*, 2004; Maritorena, Siegel, and Peterson, 2002), or EOF-based (Craig *et al.*, 2012) approaches that are capable of explicitly removing the effects of CDOM and suspended sediments from $R_{rs}(\lambda)$. Prior to applying such approaches to the WFS, however, atmospheric correction routines must continue to improve providing more accurate measures of $R_{rs}(\lambda)$ in the blue wavelengths (412 and 443 nm). Otherwise, these algorithms might also fail for coastal waters of the WFS (*e.g.* Hu *et al.*, 2003a).

Among the various research objectives of using Chl-a for climate and ecosystem related studies, a recent effort from the U.S. Environmental Protection Agency attempted to assess the nearshore (within three nautical miles of shoreline) trophic state of Florida coastal waters using satellite-derived Chl-a as an index (Schaeffer *et al.*, 2012). Anomalously high Chl-a may help resource managers make management decisions such as enacting nutrient reduction plans. The success of such an effort will depend heavily on the accuracy of satellite-based Chl-a for nearshore waters. Results here indicate that satellite-derived Chl-a in coastal waters are positively biased. Long-term trend and anomaly analyses of satellite Chl-a will require that the bias observed in empirically derived satellite Chl-a remains consistent through time; however, whether this is true cannot be determined by the limited field data presented here (*i.e.* they are spatially and temporally distributed unevenly). Thus, the success of this and future approaches that attempt to determine trophic state based on satellite-derived Chl-a in nearshore waters will depend on the continued collection of large-scale *in situ* data sets on a regular basis for algorithm refinement and validation efforts.

CONCLUSIONS

The WFS is an ecologically diverse and economically important region that can benefit greatly from routine observations from satellites to protect its many resources from such deleterious effects caused by nutrient enrichment, HABs, and weather events. Meanwhile, the optical complexity of the shallow shelf covers all possible scenarios in nature, including optically shallow, CDOM-dominant, sediment-dominant, and phytoplankton-dominant waters that might vary in both time and space. Thus, it provides an ideal region for algorithm and satellite-data product evaluations.

The results of this study indicated that while SeaWiFS Chl-a obtained offshore of the 20-m isobath were reliable, nearshore SeaWiFS Chl-a, especially within the 10-m isobath, were routinely overestimated on average by two- to fourfold. Overestimations in satellite-retrieved Chl-a in the nearshore waters of the WFS were shown to occur year round because of a variety of factors including (1) elevated CDOM associated with increased riverine discharge as during south-central Florida's

"wet season" in summer–fall and during winter–spring El Niño events; (2) sediment resuspension activity caused by winter–spring frontal and summer–fall tropical storm events; and (3) bottom reflectance in clear, shallow waters during late winter and spring after winter frontal activity subsided and before the beginning of the wet season. Together, these factors, along with HABs that typically occur in late summer and fall, all contribute to the optical complexity of the WFS on variable spatial and temporal scales, significantly influencing the magnitude and spectral variability of $R_{rs}(\lambda)$, upon which traditional empirical Chl-a algorithms are based. Several tools, including SeaWiFS ERGB composite imagery, ancillary river discharge and wind speed data, and phytoplankton cell count data provided by local, state, or federal HAB monitoring programs can be used to help determine when and where satellite-derived Chl-a should be treated with caution.

Although the influence of the previous factors on the accuracy of satellite-based Chl-a estimates has been demonstrated in other coastal waters, the study here presents a first systematic evaluation of the SeaWiFS ocean color data products on the WFS using >10 years of *in situ* data, from which the accuracy and uncertainty of the data products are quantified. Because data products from other satellite ocean color sensors such as MODIS, MERIS, and VIIRS are derived from similar algorithms, the conclusions obtained here can be extended to those sensors as well. Future Chl-a algorithm development effort for the WFS should focus on coastal waters, especially waters nearshore of the 10-m isobath, to minimize the uncertainties in Chl-a with the ultimate goal of delivering continuity of satellite-derived Chl-a across various past, current, and future missions.

ACKNOWLEDGMENTS

This work was made possible in part by a grant from BP/The Gulf of Mexico Initiative, and in part by U.S. NASA (NNX09AE17G), U.S. NOAA (NA06NES4400004), and the U.S. EPA Gulf of Mexico Program (MX-96475407-0, MX95413609-0, and MX-95453110-0). Support for field data collected during the ECOHAB program was provided by U.S. NOAA and U.S. EPA. Support for field data collected as part of NOAA-AOML's SFP was provided by the NOAA/OAR Ship Charter Fund, NOAA's Center for Sponsored Coastal Ocean Research, NOAA's Deepwater Horizon Supplemental Appropriation, and the U.S. Army Corps of Engineers. We thank NOAA NDBC for providing surface wind data and the USGS for providing river discharge data. We thank the captains and crew of the R/V Suncoaster, R/V Bellows, and R/V Walton Smith for cruise support and Lloyd Moore, David English, Daniel Otis, Merrie Beth Neely, Danylle Ault, Sue Murasko, and Julie Havens for help with sample collection and analyses. We also thank the three anonymous reviewers for providing helpful comments to improve this manuscript.

LITERATURE CITED

Ahmad, Z.; Franz, B.A.; McClain, C.R.; Kwiatkowska, E.J.; Werdell, J.; Shettle, E.P., and Holben, B.N., 2010. New aerosol models for the retrieval of aerosol optical thickness and normalized water-leaving radiances from the SeaWiFS and MODIS sensors over coastal regions and open oceans. *Applied Optics,* 49(29), 5545–5560.

Antoine, D.; d'Ortenzio, F.; Hooker, S.B.; Bécu, G.; Gentili, B.; Tailliez, D., and Scott, A.J., 2008. Assessment of uncertainty in the ocean reflectance determined by three satellite ocean color sensors (MERIS, SeaWiFS and MODIS-A) at an offshore site in the Mediterranean Sea (BOUSSOLE project). *Journal of Geophysical Research,* 113(C07013), doi: 10.1029/2007JC004472.

Bailey, S.W. and Werdell, P.J., 2006. A multi-sensor approach for the on-orbit validation of ocean color satellite data products. *Remote Sensing of Environment,* 102(1), 12–23.

Campbell, J.W., 1995. The lognormal distribution as a model for bio-optical variability in the sea. *Journal of Geophysical Research,* 100(C7), 13237–13254.

Cannizzaro, J.P. and Carder, K.L., 2006. Estimating chlorophyll *a* concentrations from remote-sensing reflectance data in optically shallow waters. *Remote Sensing of Environment,* 101(1), 13–24.

Cannizzaro, J.P.; Carder, K.L.; Chen, F.R.; Heil, C.A., and Vargo, G.A., 2008. A novel technique for detection of the toxic dinoflagellate, *Karenia brevis*, in the Gulf of Mexico from remotely sensed ocean color data. *Continental Shelf Research,* 28(1), 137–158.

Carder, K.L.; Chen, F.R.; Lee, Z.P.; Hawes, S.K., and Kamykowski, D., 1999. Semi-analytic moderate-resolution imaging spectrometer algorithms for chlorophyll *a* and absorption with bio-optical domains based on nitrate-depletion temperatures. *Journal of Geophysical Research,* 104(C3), 5403–5422.

Carder, K.L.; Hawes, S.K.; Baker, K.A.; Smith, R.C.; Steward, R.G., and Mitchell, B.G., 1991. Reflectance model for quantifying chlorophyll a in the presence of productivity degradation products. *Journal of Geophysical Research,* 96(C11), 20599–20611.

Conmy, R.N.; Coble, P.G.; Cannizzaro, J.P., and Heil, C.A., 2009. Influence of extreme storm events on West Florida Shelf CDOM distributions. *Journal of Geophysical Research,* 114(G00F04), doi: 10.1029/2009JG000981.

Craig, S.E.; Jones, C.T.; Li, W.K.W.; Lazin, G.; Horne, E.; Caverhill, C., and Cullen, J.J., 2012. Deriving optical metrics of coastal phytoplankton biomass from ocean colour. *Remote Sensing of Environment,* 119, 72–83.

Dall'Olmo, G.; Gitelson, A.A.; Rundquist, D.C.; Leavitt, B.; Barrow, T., and Holz, J.C., 2005. Assessing the potential of SeaWiFS and MODIS for estimating chlorophyll concentration in turbid productive waters using red and near-infrared bands. *Remote Sensing of Environment,* 96(2), 176–187.

Darecki, M. and Stramski, D., 2004. An evaluation of MODIS and SeaWiFS bio-optical algorithms in the Baltic Sea. *Remote Sensing of Environment,* 89(3), 326–350.

Dekker, A.G.; Phinn, S.R.; Anstee, J.; Bissett, P.; Brando, V.E.; Casey, B.; Fearns, P.; Hedley, J.; Klonowski, W.; Lee, Z.P.; Lynch, M.; Lyons, M.; Mobley, C., and Roelfsema, C., 2011. Intercomparison of shallow water bathymetry, hydro-optics, and benthos mapping techniques in Australian and Caribbean coastal environments. *Limnology and Oceanography: Methods,* 9, 396–425.

Denman, K.L. and Abbott, M.R., 1988. Time evolution of surface chlorophyll patterns from cross-spectrum analysis of satellite color images. *Journal of Geophysical Research,* 93(C6), 6789–6798.

Dogliotti, A.I.; Schloss, I.R.; Almandoz, G.O., and Gagliardini, D.A., 2009. Evaluation of SeaWiFS and MODIS chlorophyll-a products in the Argentinean Patagonian Continental Shelf (38S-55S). *International Journal of Remote Sensing,* 30(1), 251–273.

Franks, P.J.S., 1997. Spatial patterns in dense algal blooms. *Limnology and Oceanography,* 42(5), 1297–1305.

Garcia, V.M.T.; Signorini, S.; Garcia, C.A.E., and McClain, C.R., 2006. Empirical and semi-analytical chlorophyll algorithms in the southwestern Atlantic coastal region (25–40S and 60–45W). *International Journal of Remote Sensing,* 27(8), 1539–1562.

Garver, S.A. and Siegel, D.A., 1997. Inherent optical property inversion of ocean color spectra and its biogeochemical interpretation, 1, Time series from the Sargasso Sea. *Journal of Geophysical Research,* 102(C8), 18607–18625.

Gohin, F.; Druon, J.N., and Lampert, L., 2002. A five channel chlorophyll concentration algorithm applied to SeaWiFS data processed by SeaDAS in coastal waters. *International Journal of Remote Sensing,* 23(8), 1639–1661.

Gordon, H.R., 1992. Diffuse reflectance of the ocean: influence of nonuniform phytoplankton pigment profile. *Applied Optics,* 31(12), 2116–2129.

Gordon, H.R.; Brown, O.B., and Jacobs, M.M., 1975. Computed relationships between the inherent and apparent optical properties of a flat homogenous ocean. *Applied Optics,* 14(2), 417–427.

Gregg, W.W. and Conkright, M.E., 2002. Decadal changes in global ocean chlorophyll. *Geophysical Research Letters,* 29(15), doi: 10.1029/2002GL014689.

Holm-Hansen, O.; Lorenzen, C.J.; Holmes, R.W., and Strickland, J.D.H., 1965. Fluorometric determination of chlorophyll. *Journal du Conseil*, *Conseil Permanent International pour l'Exploration de la Mer,* 30(1), 3–15.

Hu, C., 2008. Ocean color reveals sand ridge morphology on the West Florida Shelf. *IEEE Geoscience and Remote Sensing Letters,* 5(3), 443–447.

Hu, C.; Carder, K.L., and Müller-Karger, F.E., 2000. Atmospheric correction of SeaWiFS imagery over turbid coastal waters: a practical method. *Remote Sensing of Environment,* 74(2), 195–206.

Hu, C.; Lee, Z.P.; Müller-Karger, F.E., and Carder, K.L., 2003a. Application of an optimization algorithm to satellite ocean color imagery: A case study in Southwest Florida coastal waters. *In:* Frouin, R.J.; Yuan, Y., and Kawamura, H. (ed.), *Ocean Remote Sensing and Applications*. Bellingham, Washington: SPIE, pp. 70–79.

Hu, C.; Luerssen, R.; Müller-Karger, F.E.; Carder, K.L., and Heil, C.A., 2008. On the remote monitoring of *Karenia brevis* blooms of the west Florida shelf. *Continental Shelf Research,* 28(1), 159–176.

Hu, C.; Müller-Karger, F.E.; Biggs, D.C.; Carder, K.L.; Nababan, B.; Nadeau, D., and Vanderbloemen, J., 2003b. Comparison of ship and satellite bio-optical measurements on the continental margin of the NE Gulf of Mexico. *International Journal of Remote Sensing,* 24(13), 2597–2612.

Hu, C.; Müller-Karger, F.E.; Taylor, C.; Carder, K.L.; Kelble, C.; Johns, E., and Heil, C.A., 2005. Red tide detection and tracing using MODIS fluorescence data: an example in SW Florida coastal waters. *Remote Sensing of Environment,* 97(3), 311–321.

Hyde, K.J.W.; O'Reilly, J.E., and Oviatt, C.A., 2007. Validation of SeaWiFS chlorophyll a in Massachusetts Bay. *Continental Shelf Research,* 27(12), 1677–1691.

Le, C.; Hu, C.; Cannizzaro, J.; English, D.; Müller-Karger, F., and Lee, Z., 2013a. Evaluation of chlorophyll-a remote sensing algorithms for an optically complex estuary. *Remote Sensing of Environment*, 129, 75–89.

Le, C.; Hu, C.; English, D.; Cannizzaro, J., and Kovach, C., 2013b. Climate driven chlorophyll-a changes in a turbid estuary: observations from satellites and implications for management. *Remote Sensing of Environment*, 130, 11–24.

Lee, Z.; Ahn, Y.; Mobley, C., and Arnone, R., 2010. Removal of surface-reflected light for the measurement of remote-sensing reflectance from an above-surface platform. *Optics Express,* 18(25), 26313–26324.

Lee, Z.; Carder, K.L., and Arnone, R.A., 2002. Deriving inherent optical properties from water color: a multiband quasi-analytical algorithm for optically deep waters. *Applied Optics,* 41(27), 5755–5772.

Lee, Z.; Carder, K.L.; Mobley, C.D.; Steward, R.G., and Patch, J.S., 1999. Hyperspectral remote sensing for shallow waters: 2. Deriving bottom depths and water properties by optimization. *Applied Optics,* 38(18), 3831–3843.

Lyon, P.E.; Hoge, F.E.; Wright, C.W.; Swift, R.N., and Yungel, J.K., 2004. Chlorophyll biomass in the global oceans: satellite retrieval using inherent optical properties. *Applied Optics,* 43(31), 5886–5892.

Maritorena, S.; Siegel, D.A., and Peterson, A.R., 2002. Optimization of a semi-analytical ocean color model for global-scale applications. *Applied Optics,* 41(15), 2705–2714.

McClain, C.R.; Feldman, G.C., and Hooker, S.B., 2004. An overview of the SeaWiFS project and strategies for producing a climate research quality global ocean bio-optical time series. *Deep Sea Rearch II,* 51(1), 5–42.

Melin, F.; Zibordi, G., and Berthon, J., 2007. Assessment of satellite ocean color products at a coastal site. *Remote Sensing of Environment,* 110(2), 192–215.

Morel, A., 1988. Optical modeling of the upper ocean in relation to its biogenous matter content (Case I waters). *Journal of Geophysical Research,* 93(C9), 10749–10768.

Morel, A. and Prieur, L., 1977. Analysis of variations in ocean color. *Limnology and Oceanography,* 22(4), 709–722.

Morey, S.L.; Dukhovskoy, D.S., and Bourassa, M.A., 2009. Connectivity between variability of the Apalachicola River flow and the biophysical oceanic properties of the northern West Florida Shelf. *Continental Shelf Research,* 29(9), 1264–1275.

Nababan, B., 2005. Bio-optical Variability of Surface Waters in the Northeastern Gulf of Mexico. St. Petersburg, Florida: University of South Florida, Doctoral dissertation, 158 p.

Nababan, B., 2010. Comparison of chlorophyll concentration estimation using two different algorithms and the effect of colored dissolved organic matter. *International Journal of Remote Sensing and Earth Sciences,* 5(1), 92–101.

O'Reilly, J.E.; Maritorena, S.; Siegel, D.A.; O'Brien, M.C.; Toole, D.; Mitchell, B.G.; Kahru, M.; Chavez, F.P.; Strutton, P.; Cota, G.F.; Hooker, S.B.; McClain, C.R.; Carder, K.L.; Müller-Karger, F.; Harding, L.; Magnuson, A.; Phinney, D.; Moore, G.F.; Aiken, J.; Arrigo, K.R.; Letelier, R., and Culver, M., 2000. Ocean color chlorophyll *a* algorithms for SeaWiFS, OC2, and OC4: Version 4. *In:* Hooker, S.B. and Firestone, E.R. (eds.), *SeaWiFS Postlaunch Calibration and Validation Analyses, Part 3*. Greenbelt, Maryland: NASA Goddard Space Flight Center, pp. 9–23.

Ruddick, K.G.; Ovidio, F., and Rijkeboer, M., 2000. Atmospheric correction of SeaWiFS imagery for turbid coastal and inland waters. *Applied Optics,* 39(6), 897–912.

Schaeffer, B.A.; Hagy, J.D.; Conmy, R.N.; Lehrter, J.C., and Stumpf, R.P., 2012. An approach to developing numeric water quality criteria for coastal waters using the SeaWiFS satellite data record. *Environmental Science & Technology,* 46(2), 916–922.

Schmidt, N.; Lipp, E.K.; Rose, J.B., and Luther, M.E., 2001. ENSO influences on seasonal rainfall and river discharge in Florida. *Journal of Climate,* 14(4), 615–628.

Shoaf, W.T. and Lium, B.W., 1976. Improved extraction of chlorophyll a and b from algae using dimethyl sulfoxide. *Limnology and Oceanography,* 21(6), 926–928.

Siegel, D.A.; Wang, M.; Maritorena, S., and Robinson, W., 2000. Atmospheric correction of satellite ocean color imagery: the black pixel assumption. *Applied Optics,* 39(21), 3582–3591.

Stumpf, R.P.; Arnone, R.A.; Gould, R.W.; Martinolich, P.; Ransibrahmanakul, V.; Tester, P.A.; Steward, R.G.; Subramaniam, A.; Culver, M.E., and Pennock, J.R., 2000. SeaWiFS ocean color data for US Southeast coastal waters. *In: Proceedings of the Sixth International Conference on Remote Sensing for Marine and Coastal Environments*. (Ann Arbor, Michigan, Veridian ERIM International), pp. 25–27.

Stumpf, R.P.; Arnone, R.A.; Gould, R.W.; Martinolich, P.M., and Ransibrahmanakul, V., 2003a. A partially coupled ocean-atmosphere model for retrieval of water-leaving radiance from SeaWiFS in coastal waters. *In:* Hooker, S.B. and Firestone, E.R. (eds.), *NASA Tech. Memo. 2003–206892, Volume 22*. Greenbelt, Maryland: NASA Goddard Space Flight Center, pp. 51–59.

Stumpf, R.P.; Culver, M.E.; Tester, P.A.; Tomlinson, M.; Kirkpatrick, G.J.; Pederson, B.A.; Truby, E.; Ransibrahmanakul, V., and Soracco, M., 2003b. Monitoring *Karenia brevis* blooms in the Gulf of Mexico using satellite ocean color imagery and other data. *Harmful Algae,* 2(1), 147–160.

Stumpf, R.P. and Pennock, J.R., 1989. Calibration of a general optical equation for remote sensing of suspended sediments in a moderately turbid estuary. *Journal of Geophysical Research,* 94(C10), 14363–14371.

Subramaniam, A.; Brown, C.W.; Hood, R.R.; Carpenter, E.J., and Capone, D.G., 2002. Detecting *Trichodesmium* blooms in SeaWiFS imagery. *Deep-Sea Research II,* 49(1), 107–121.

Thuillier, G.; Herse, M.; Simon, P.C.; Labs, D.; Mandel, H.; Gillotay, D., and Foujols, T., 2003. The solar spectral irradiance from 200 to

2400 nm as measured by the SOLSPEC spectrometer from the ATLAS 1-2-3 and EURECA missions. *Solar Physics,* 214(1), 1–22.

Udy, J.; Gall, M.; Longstaff, B.; Moore, K.; Roelfsema, C.; Spooner, D.R., and Albert, S., 2005. Water quality monitoring: a combined approach to investigate gradients of change in the Great Barrier Reef, Australia. *Marine Pollution Bulletin,* 51(1), 224–238.

Vargo, G.A.; Heil, C.A.; Fanning, K.A.; Dixon, L.K.; Neely, M.; Lester, K.; Ault, D.; Murasko, S.; Havens, J.; Walsh, J., and Bell, S., 2008. Nutrient availability in support of *Karenia brevis* blooms on the central West Florida Shelf: what keeps *Karenia* blooming? *Continental Shelf Research,* 28(1), 73–98.

Walsh, J.J.; Jolliff, J.K.; Darrow, B.P.; Lenes, J.M.; Milroy, S.P.; Remsen, A.; Dieterle, D.A.; Carder, K.L.; Chen, F.R.; Vargo, G.A.; Weisberg, R.H.; Fanning, K.A.; Müller-Karger, F.E.; Shinn; E., Steidinger, K.A.; Heil, C.A.; Tomas, C.R.; Prospero, J.S.; Lee, T.N.; Kirkpatrick, G.J.; Whitledge, T.E.; Stockwell, D.A.; Villareal, T.A.; Jochens, A.E., and Bontempi, P.S., 2006. Red tides in the Gulf of Mexico: where, when and why? *Journal of Geophysical Research,* 111(C11003), doi: 10.1029/2004JC002813.

Wang, M. and Shi, W., 2007. The NIR-SWIR combined atmospheric correction approach for MODIS ocean color data processing. *Optics Express,* 15(24), 15722–15733.

Weisberg, R.H.; He, R.; Kirkpatrick, G.; Müller-Karger, F., and Walsh, J.J., 2004. Coastal ocean circulation influences on remotely sensed optical properties: a west Florida shelf case study. *Oceanography,* 17(2), 68–75.

Werdell, P.J.; Bailey, S.W.; Franz, B.A.; L.W.; Jr., Harding, Feldman, G.C., and McClain, C.R., 2009. Regional and seasonal variability of chlorophyll-a in Chesapeake Bay as observed by SeaWiFS and MODIS-Aqua. *Remote Sensing of Environment,* 113(6), 1319–1330.

Wozniak, S.B. and Stramski, D., 2004. Modeling the optical properties of mineral particles suspended in seawater and their influence on ocean reflectance and chlorophyll estimation from remote sensing algorithms. *Applied Optics,* 43(17), 3489–3503.

Yoder, J.A. and Kennelly, M.A., 2003. Seasonal and ENSO variability in global ocean phytoplankton chlorophyll derived from 4 years of SeaWiFS measurements. *Global Biogeochemical Cycles,* 17(4), doi: 10.1029/2002GB001942.

Zibordi, G.; Melin, F., and Berthon, J.F., 2006. Comparison of SeaWiFS, MODIS, and MERIS radiometric products at a coastal site. *Geophysical Research Letters,* 33(L06617), doi: 10.1029/2006GL025778.